

Supplementary Information

Uniform $\text{MnCo}_2\text{O}_{4.5}$ porous nanowires and quasi-cubes for hybrid supercapacitors with excellent electrochemical performances

Xuming Du, Jiale Sun, Runze Wu, Enhui Bao, Chunju Xu*, Huiyu Chen*

School of Materials Science and Engineering, North University of China, Taiyuan 030051, China

* Corresponding authors.

E-mail: chunju@nuc.edu.cn (C. Xu); hychen@nuc.edu.cn (H. Chen)

S1. Structural characterizations of the electrode materials

The crystallographic structure was characterized by X-ray diffraction (XRD), which was performed on a diffractometer (Bruker D8 Advance) and Cu-K α with wave length of 0.15418 nm was employed as radiation. The surface morphologies were observed using a scanning electron microscope (SEM, JEOL JSM7100F). The energy dispersive X-ray spectroscopy (EDS) elemental mappings were also acquired through the same equipment. Transmission electron microscopy (TEM) image, high-resolution TEM (HRTEM) image, and corresponding selected-area electron diffraction (SAED) analysis were carried out to investigate the detailed microstructures on JEOL JEM2100F equipment with an accelerating voltage of 200 kV. X-ray photoelectron spectroscopy (XPS) was conducted on an ESCA 2000 spectrometer to study the elemental valence states. The specific surface area and the pore size distribution of the products were acquired from the N₂ adsorption-desorption isotherms at 77 K with a Quantachrome Autosorb 1-C absorption analyzer, and the Brunauer-Emmett-Teller (BET) and Barret-Joyner-Halenda (BJH) models were employed in the calculation process.

S2. Electrochemical tests using three-electrode method

To evaluate electrochemical performance of porous MnCo₂O_{4.5} NWs, cyclic voltammetry (CV) curves, galvanostatic charge-discharge (GCD) curves, and electrochemical impedance spectrum (EIS) were recorded on an electrochemical workstation (CHI 660E, Shanghai Chenhua, China) using a three-electrode configuration in 2 M KOH electrolyte. The counter electrode and reference electrode were based on Pt foil and Hg/HgO, respectively. To fabricate working electrode, the grass-like MnCo₂O_{4.5} NWs were scraped from SSF substrate, and mixed with acetylene black and polyvinylidene fluoride (PVDF) binder in a mass ratio of 80:15:5. The powdered mixture was dispersed in *N*-methyl-2-pyrrolidone (NMP) to form black homogeneous slurry. Then we coated the slurry on clean Ni foam and processed vacuum-drying at 105 °C for 12 h. The nickel foam loaded with MnCo₂O_{4.5} NWs was eventually pressed using a pressure of 10 MPa, and the loading weight of MnCo₂O_{4.5} NWs was measured to be 2.6 mg. Under the operating potential windows of 0 ~ 0.75 and 0 ~ 0.55 V, CV measurements

were performed at various scan rates from 5 to 50 mV s⁻¹ and GCD measurements were conducted under different current densities varying from 1 ~ 8 A g⁻¹, respectively. EIS was evaluated over the frequency range from 0.01 Hz to 100 kHz.

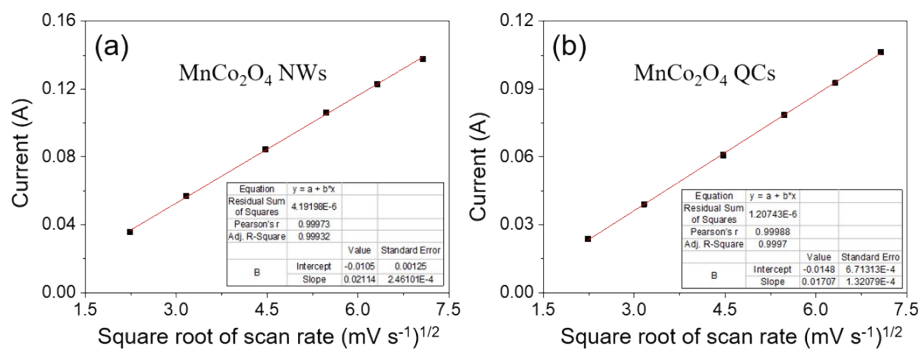


Figure S1. The curves of anode peak current density as a function of square root of scan rate for (a) MnCo_2O_4 NWs and (b) MnCo_2O_4 QCs.

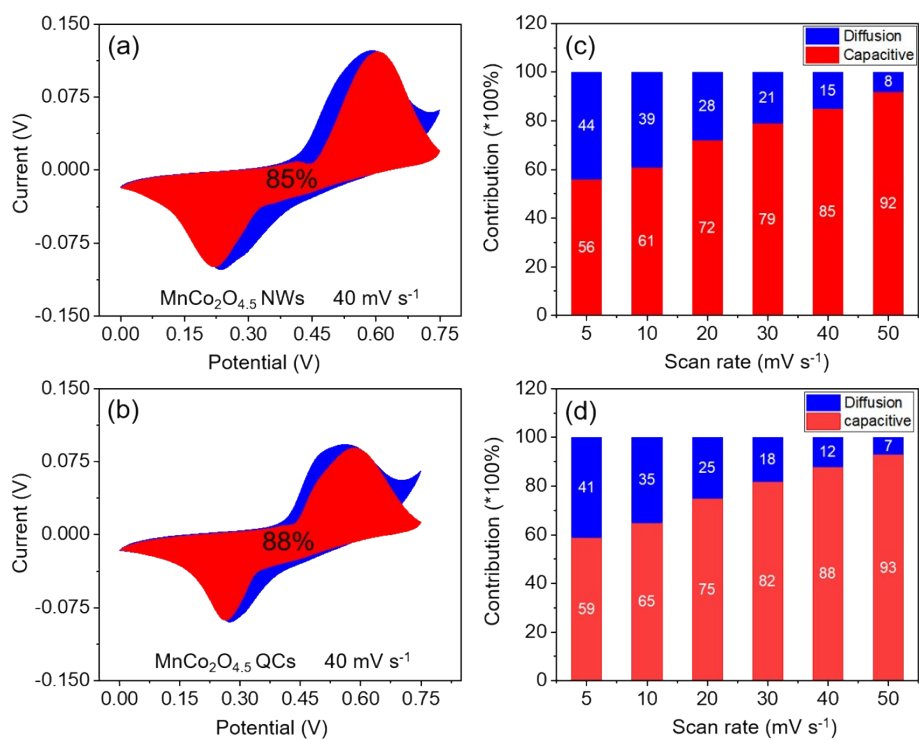


Figure S2. Kinetics and quantitative analysis of the storage mechanism: capacitive (red) and diffusion-controlled (blue) contributions to the total charge storage of (a) MnCo₂O_{4.5} NWs and (b) MnCo₂O_{4.5} QCs at 40 mV s⁻¹, and normalized contribution ratio of capacitive (red) and diffusion-controlled (blue) capacities for (c) MnCo₂O_{4.5} NWs and (d) MnCo₂O_{4.5} QCs at different scan rates.

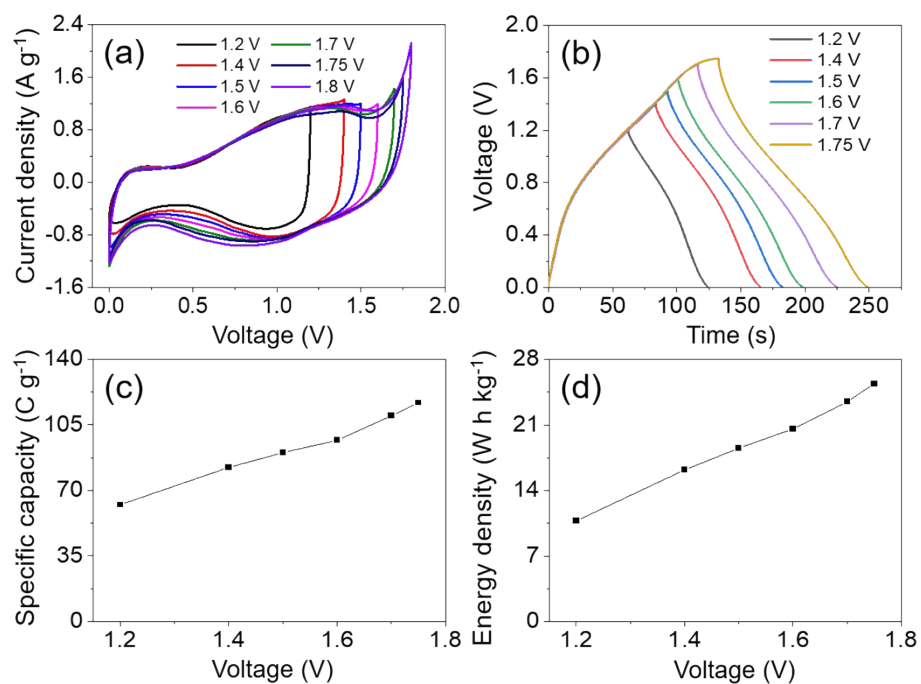


Figure S3. (a) CV curves of the MnCo₂O_{4.5} NWs//AC HSC over different voltage windows at the scan rate of 10 mV s⁻¹, (b) GCD curves of the MnCo₂O_{4.5} NWs//AC HSC over different voltage windows at 1 A g⁻¹, (c) the relationship of specific capacity vs voltage window for MnCo₂O_{4.5} NWs//AC HSC, and (d) the energy density of MnCo₂O_{4.5} NWs//AC HSC as a function of voltage window. The capacity in (c) and energy density in (d) were obtained at the current density of 1 A g⁻¹.